JOURNAL OF MATERIALS SCIENCE 14 (1979) 2941–2958

The formation and properties of mineral-polyacid cements

Part 1 *Ortho- and pyro-silicates*

STEPHEN CRISP, SHEILA MERSON, ALAN D. WILSON
Laboratory of the Government Chemist, Cornwall House, Stamford Street, London SE1 9NQ, UK

JOSEPH H. ELLIOTT, PETER R. HORNSBY
Department of Non-Metallic Materials, Brunel University, Kingston Lane, Uxbridge, Middlesex, UK

A study of the cement-forming reactions between certain naturally occurring *ortho-* and *pyro*-silicate minerals and aqueous polyacid solutions is presented with particular reference to the rheological characteristics of the cement mixtures and the mechanical properties of the hardened cement pastes. The hydrolytic stability of the cements is discussed in terms of the nature of cations present in the gel matrix.

1. Introduction

Hard ceramic-like materials, generically termed "ionic polymer cements", are formed as a result of the reaction between powders of certain metal oxides, glasses or silicate minerals, and aqueous solutions of poly(acrylic acid) (PAA) or related polyacids [1, 2]. The reaction depends on the ability of the inorganic component to release cations in the presence of the acid and of the liberated cations to bind with polyanion chains in solution to yield an insoluble gel. The resulting product has a composite microstructure of incompletely reacted powder particles set in a hydrated polysalt matrix.

Of the many cement-forming systems which have been studied only two – zinc polycarboxylate and ASPA cements – have achieved commercial significance and both have found application so far only in the field of dentistry. Of these, the zinc polycarboxylate cement is prepared from an intimate mixture of zinc oxide and an aqueous solution of poly(acrylic acid) or a co-polymer of acrylic and itaconic acids [3, 4]. In the glass ionomer or ASPA cement, however, the powder phase is replaced by an aluminosilicate, fluoro-aluminosilicate, or phosphate aluminosilicate glass of closely controlled composition [5]. Extra-dental biomedical and sand binding applications for this material are currently under evaluation. Detailed investigations of its formation and properties have been reported elsewhere [1, 6–9].

In a preliminary communication, an account was given of the reactions which occur between various acid-soluble silicate minerals and solutions of polysulphonic and polycarboxylic acids [10]. Many of the compositions investigated set to crumbly, plastic or rubbery solids of low compressive strength and limited hydrolytic stability, although some showed greater promise as useful materials and warranted more detailed studies. Furthermore, such investigations using well-characterized minerals of known structure could increase the fundamental understanding of this class of material.

This paper reports on the reactions of selected *ortho-* and *pyro*-silicate minerals with aqueous solutions of PAA and a co-polymer of itaconic and acrylic acids. Instrumental techniques, including arc emission spectroscopy, X-ray diffraction (XRD) and differential thermal analysis (DTA), were used to assess mineral purity and the size distributions of powder samples were compared using a Coulter Counter. The early stages of the cement-forming reaction, involving acid-

0022–2461/79/122941–18$03.80/0 © *1979 Chapman and Hall Ltd.*

decomposition of mineral powders, were monitored by chemical analysis of the soluble ion extracts from a suspension of the powders in dilute PAA solution. The extent of mineral erosion was estimated from changes in line intensities of X-ray powder diffraction patterns. This method was complemented by a qualitative measure of the incidence of polysalt formation determined from infra-red spectra of hardened cements. The setting behaviour of cement mixtures was followed using both rheometric and penetrometer techniques. Mechanical properties and solubilities of hardened cements were measured by standard procedures.

2. Experimental details

Naturally occurring *ortho-* and *pyro*-silicate minerals (Table I), were chosen for more-detailed investigation on the basis of their known reactivity towards polyacid solutions and their potential as useful cement formers. Bulk samples were ground to pass through a 38 μm test sieve, and their elemental composition estimated semi-quantitatively by arc emission spectroscopy across graphite electrodes. Further evidence of mineral purity was obtained from Debye–Scherrer X-ray diffraction patterns using Cu$K\alpha$ radiation passed through a Ni filter. An exposure time of 7 h was found to be satisfactory for all of the minerals except gadolinite which required a minimum of 24 h exposure before a discernible pattern was produced. Calculated interplanar (d) spacings and estimated line intensities were compared with corresponding ASTM powder diffraction data. Differential thermal analysis curves were also recorded for the mineral powders up to 1000° C at a heating rate of 10° C min^{-1}, using calcined alumina as inert reference material and in some cases as a sample diluent to reduce base-line drift.

The particle size distribution of a representative sample from each of the mineral powders was determined using a Model D Industrial Coulter Counter fitted with a 140 μm aperture tube. An aqueous solution of 4% m/m* tetrasodium pyrophosphate was employed as supporting electrolyte. Mineral densities were measured by pyknometry on powdered samples.

Aqueous poly(acrylic acid) solution was chosen as the preferred acid for this study, since it was thought to react with all of the selected minerals, and to form hydrolytically stable cements with many of them. Furthermore, this polyacid has been widely used in fundamental studies on analogous ionic polymer cements thus facilitating comparison of results with these systems. The PAA solution was prepared by the aqueous polymerization of acrylic acid using ammonium persulphate as initiator and propan-2-ol as chain transfer agent. Viscosity stabilizing additives and setting time modifiers, which are sometimes included in glass-ionomer cement formulations, were not added. The aqueous polyacid solution was concentrated to 50% m/m by vacuum distillation. For some experiments, notably setting time and mechanical property studies, cements were also made from a co-polymer of acrylic and itaconic acids, in an attempt to improve their manipulative and hardening characteristics.

The initial stages of the reaction between the mineral powders and PAA solution were studied in a model system. Weighed amounts of powder were shaken with a measured volume of diluted PAA solution (0.5% m/m) for 1 h. The suspensions were then centrifuged and the aqueous phase decanted from the sediment for chemical analysis. Semi-quantitative ultra-violet emission spectrography was used initially for this purpose, as a rough screen, followed by more accurate determination of the concentration of selected elements by atomic absorption spectrophotometry, although this was not possible for sodium and aluminium as lamps for these elements were not available. A parallel set of measurements was also obtained from the dilute PAA solution free from mineral extracts.

In order to ascertain the extent of mineral decomposition, weighed quantities of the mineral powders were suspended in a 1% m/m aqueous PAA solution with occasional shaking for 1 week at 23° C. Mixtures were then centrifuged, and the mineral residues dried at 60° C. These were analysed by the X-ray diffraction procedures previously described.

KBr disc transmission infra-red spectra were recorded for hardened mineral–PAA cement mixtures over the frequency range 2000 to 800 cm^{-1}. Spectra of the parent minerals in isolation were obtained in the same way.

The approximate setting times of mineral–PAA cement mixtures were determined initially using a 450 g Gillmore type needle according to

*m/m = mass/mass.

TABLE I Spectrographic analysis of silicate minerals

Mineral	Formula [21]	Supplier	Elements detected																		
			Fe	Si	Mg	Ca	Na	K	Al	Mn	Zn	Ti	Sn	Ni	As	V	Mo	Sb	B	Cr	Cu	Yb
Andradite	$Ca_3Fe_2(SiO_4)_3$	A	M	M	m	M	m		m	t	t	t	t									
Gadolinite	$Be_2FeY_2O_2(SiO_4)_2$	D	M	M	t	t		m	m	t												
Gehlenite	$Ca_2Al_2SiO_7$	B	m	M	M	M	m	m	M	t		t										
Hardystonite	$Ca_2ZnSi_2O_7$	B	m	M	m	M	Ob		m	t	M											
Hemimorphite	$Zn_4Si_2O_7(OH)_2 \cdot H_2O$	A	M	M	m	m	Ob		t	m	M				m	t	t	t				
Olivine	$(Mg, Fe)_2SiO_4$	C	M	M	M		t		t	t	t			t						t	t	
Spurrite	$Ca_5Si_2O_8CO_3$	A	m	M	m	M	t		m	t		t				t			t	t	t	
Tephroite	Mn_2SiO_4	A	M	M	M	t		m	m	M	t	t		t		t				t	t	t
Willemite	Zn_2SiO_4	B	M	M	M	t	Ob		m	M	M									t	t	t

M = major (> 5%); m = minor (0.1 to 5%); t = trace (< 0.1%); Ob = obscured.

A = R.F.D. Parkinson Co Ltd., Doulting, Shepton Mallet, Somerset, UK.

B = Wards Natural Science Establishment Rochester, New York, USA.

C = Gemstones, Hatton Gardens, London, UK.

D = Laboratory of the Government Chemist Sample Museum, London, UK.

the procedure laid down in BS 3365 [11], except that tests were carried out at 23° C and room humidity (70 to 80% r.h.). In most compositions a 2/1 wt/vol powder-to-liquid ratio was used, although in the case of minerals of high reactivity it was necessary to use a 1/1 wt/vol ratio instead. A more complete understanding of the setting behaviour of these systems in terms of available manipulation time, setting time and post-set hardening rate, was obtained using an oscillating rheometer [12].

Cylindrical compressive strength specimens were prepared from mineral–PAA cement mixtures in stainless steel split moulds constructed according to BS 3365 recommendations [11]. Ratios of powder-to-liquid in these compositions were the same as for the setting time studies; however, since the cement pastes reacted and set at different rates, hardened test pieces were removed from their moulds at times ranging between 1 and 24 h from the commencement of mixing. Since the mixture containing olivine had not hardened after a week, mechanical property measurements on this system were abandoned. After removal from the moulds all specimens were stored at 100% r.h. (23° C) until they had aged for a total of 7 days from the start of mixing. Half of each set of samples were then immersed in distilled water at 23° C at 7 days, whereas the remainder were maintained at 100% r.h. (23° C) for a further period of 7 days. Following storage, all samples were tested to failure in compression on an Instron testing machine using a cross-head speed of 0.5 mm min^{-1}. From these results and dimensions of the original specimens, average values of compressive strength, strain at failure and modulus of elasticity (in compression), taken as the ratio of ultimate stress to strain, were calculated.

Solubility discs, 20 mm diameter, were prepared according to BS 3365 [11], the moulds being sealed and clamped for 24 h at 23° C. Cement discs were then removed and stored at 100% r.h. (23° C) for 7 days, followed by another 7 days in double deionized water at 23° C. After removal of the cement specimens the water was transferred to a weighed bottle and evaporated to dryness. Percentage solubility was determined from the increase in weight of the bottle.

3. Results

Spectrographic analyses of the silicate minerals used in this investigation are shown in Table I, in terms of major (>5%), minor (0.1 to 5%) and trace (<0.1%) amounts of each element present. From an interpretation of their XRD patterns the purity of each mineral was assessed. These inferences and the probable nature of impurities are presented in Table II. Results from DTA studies, shown in Fig. 1 and Table III, provide little additional evidence of mineral composition. Wherever possible, temperatures of principal energy changes are compared with corresponding data reported in the literature, although the reliability of this information is questionable due to the considerable variation in published results for different sources of the same mineral.

Particle size distributions of mineral powders are compared in Fig. 2 and the specific surface area values of the powders are given in Table IV. The latter were calculated using measured mineral densities, assuming a spherical particle shape.

The concentration of ions extracted from the mineral powders during the early stages of reaction with dilute PAA solution is recorded in Table V. Semi-quantitative values from the initial ultraviolet emission analysis are also included in parentheses. To assist in the interpretation of these results, the soluble ion concentration has been arbitrarily classified into major and minor amounts (Table VI).

Complementary studies to determine the incidence of mineral decomposition after 1 week in contact with an excess dilute PAA solution indicated that with all mineral residues changes in X-ray diffraction intensities occurred, but to differing degrees.

The infra-red spectra of mineral–PAA mixtures and also the parent minerals are shown in Fig. 3, with their band assignments listed in Table VII. An important feature of these cement spectra is the appearance of absorptions at approximately 1550 and 1410 cm^{-1}, associated with the asymmetric and symmetric stretching modes of metal–polyacrylate salts. The extent of reaction in the mixtures may be estimated from the decrease in intensity (or total disappearance) of the band at about 1700 cm^{-1}, assigned to the acid carbonyl group.

Results defining the rheological behaviour of freshly prepared mineral–PAA cement mixtures are given in Table VIII and Fig. 4. Experimental limitations of the Gillmore needle penetrometer permit only an approximate measurement of a cement's setting time. The oscillating rheometer

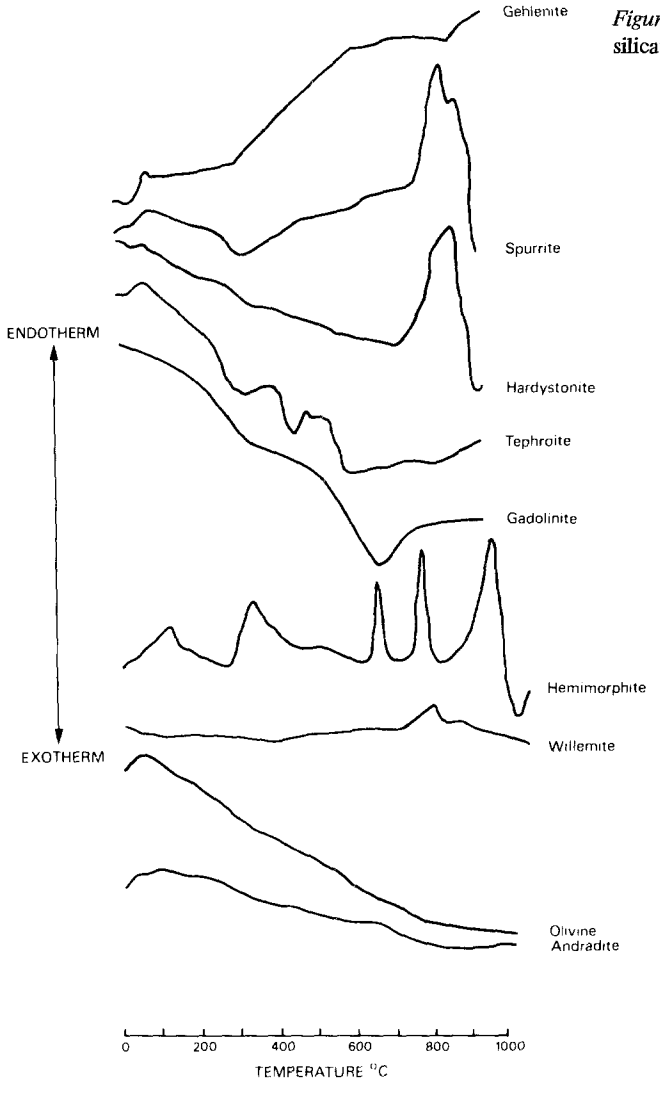

Figure 1 Differential thermal analysis of silicate minerals (heating rate 10° C min^{-1})

is more versatile, however, and provides a continuous record of stiffness against time. Traces of this type are generally characterized by three regions [20]: an initial region where the cement paste is workable and the amplitude remains constant at a maximum value; an intermediate region where the cement mixture thickens and the rate of decrease of amplitude reaches a maximum; and a final region where a constant but small amplitude is obtained as the cement sets. To aid practical distinction between these three stages of behaviour, for the purposes of this investigation,

TABLE II Determination of mineral purity by X-ray diffraction

Mineral	Composition
Andradite	Andradite identified with trace amounts of α-quartz impurity
Gadolinite	Gadolinite identified (pattern very weak)
Gehlenite	Gehlenite present with akermanite ($Ca_2MgSi_2O_7$) impurity
Hardystonite	Only hardystonite present
Hemimorphite	Hemimorphite identified with very small quantities of an unidentified impurity
Olivine	Only olivine present
Spurrite	Spurrite present with large amounts of calcite ($CaCO_3$) impurity
Tephroite	Mixture of tephroite with impurity minerals
Willemite	Mixture of willemite possibly troostite and franklinite $(Zn, Mn, Fe)O(FeMn)_2O_3$

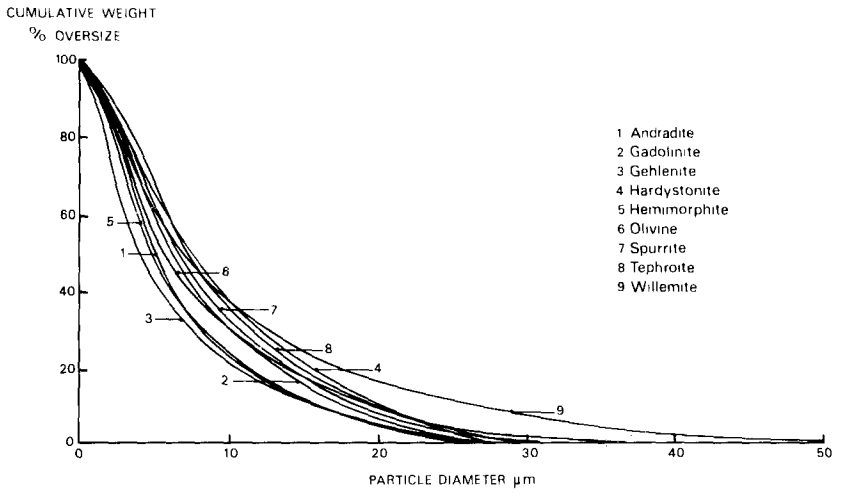

Figure 2 Particle size distribution of silicate minerals.

the available working time was defined as the point in time at which the amplitude of the oscillation was reduced to 90% of its original value. A cement was considered to have set when the envelope of the trace approached the abscissa and became linear.

TABLE III Differential thermal analysis of silicate minerals

Mineral	Principal peaks (° C)	Literature data (° C)	Reference
Andradite	80 vs– 750 bvs+?		
Gadolinite	675 bm+	470 bs+ 850 ms+	[13]
Gehlenite	85 s– 320 bs+ 600 bm– 850 s+		
Hardystonite	75 s– 865 bl–		
Hemimorphite	110 bms– 300 bm– 580 m– 673 ml– 840 ml– 900 ms+	660 ms– 670 ms– 705 m– 740 ms– 850 ms+ 925 ms+ 937 ms+ 971 ms+	[14–17]
Olivine	50 bs–	200 (s) vs– 690 vs–	[15]
Spurrite	100 bs– 350 bms+ 840 l– 885 l–	< 500 various vs– 725–850 l– 845–990 l–	[18]
Tephroite	80 vs– 285 vs+ 340 s+ 450 ms+ 510 vs+ 600 bm+		
Willemite	790 s–	337 s+ 675 m–	[19]

l = large; ml = medium large; m = medium; ms = medium small; s = small; vs = very small.
+ = exotherm; – = endotherm; b = broad; (s) = exceptionally sharp peak; ? = peak uncertain.

TABLE IV Specific surface area and density of silicate minerals

Mineral	Density ($Mg\ m^{-3}$)	Specific surface area ($m^2\ g^{-1}$)
Andradite	3.49	4.15
Gadolinite	3.8	3.94
Gehlenite	2.62	3.2
Hardystonite	3.15	2.99
Hemimorphite	3.6	4.2
Olivine	3.13	3.68
Spurrite	2.81	2.76
Tephroite	3.76	3.69
Willemite	4.39	4.11

Differences in powder-to-liquid ratio and the hydrolytic instability of many of the cements prevents a true comparison of their mechanical properties under the test conditions employed (Table IX). Cements made from gadolinite and willemite were strongest and stiffest but the compressive strength and values for modulus of elasticity in compression compared unfavourably with glass-ionomer and zinc polycarboxylate dental cements. Several coments appeared hydrolytically stable in qualitative tests and were only slightly soluble in deionized water. Compositions containing gehlenite and spurrite softened when immersed in water and were characterized by a high strain at failure.

4. Discussion

4.1. Characterization of minerals

A comparison of the elemental composition of minerals used in this study with their theoretical formulae (Table I), shows that all of the samples contained trace amounts of naturally occurring impurity elements, relating to their origin. The XRD patterns (Table II) and spectrographic analyses (Table I), of the mineral show the samples of hardystonite and olivine to be relatively pure. Andradite and hemimorphite, on the other hand, contain small amounts of α-quartz and an unidentified iron-rich impurity, respectively. Significant quantities of akermanite ($Ca_2MgSi_2O_7$) were identified together with gehlenite, suggesting that this sample was an isomorphous mixture of these minerals, perhaps melilite [21]. Similarly, large amounts of calcite ($CaCO_3$) impurity were found with spurrite. Mixtures of these substances

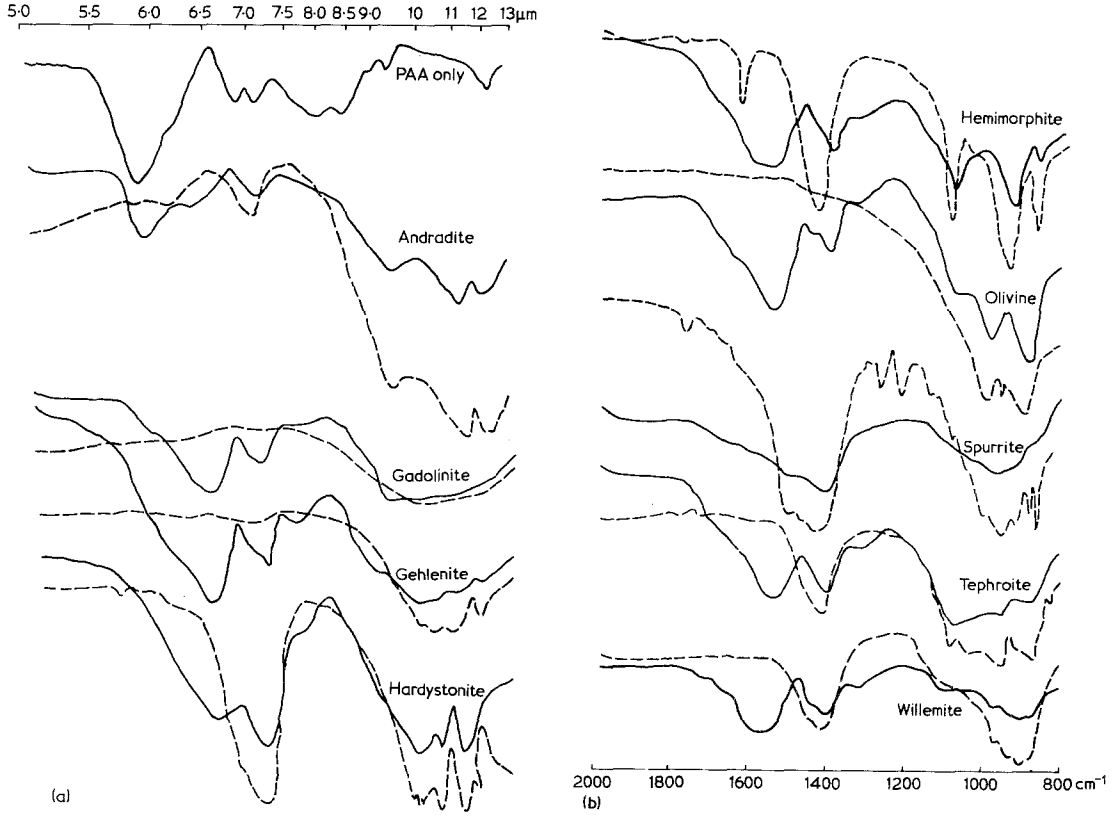

Figure 3 Infra-red spectra of: silicate minerals - - - -; silicate minerals + PAA solutions pastes ———

TABLE V Chemical analysis of silicate mineral extracts ($\mu g\ ml^{-1}$) by atomic absorption and ultra-violet emission spectroscopy

Mineral	Al	Be	Ca	Cd	Cr	Cu	Fe	Mg	Mn	Na	Ni	Pb	Sn	Zn	B	Si
Andradite		–	26.5	< dl	< dl	1.65	15.5	16.0	1.1		< dl	< dl		1.49		34.5
	(10)		(> 10)	(tr)	–	(10)	(100)	(10)	(< 10)		–	(tr)	–	(10)	(< 10)	(100)
Gadolinite			4.9	< dl	< dl	1.60	15.6	7.3	3.4		< dl	12.6		31.2		100
	(> 10)	(10)	(100)	(tr)	–	(10)	(100)	(10)	(10)	(tr)	(tr)	(> 10)	–	(100)	(10)	(100)
Gehlenite			75.0	< dl	0.1	0.4	8.0	49.5	0.7		< dl	0.26		31.3		200
	(100)	–	(100)	(tr)	–	(> 10)	(100)	(100)	(< 10)	(100)	–	(10)	–	(100)	(10)	(> 100)
Hardystonite			165.0	< dl	< dl	0.2	< dl	1.85	3.22		< dl	1.62		1.61		600
	(< 10)	–	(100)	(tr)	–	(< 10)	(tr)	(10)	(10)	(100)	–	(10)	–	(100)	(10)	(> 100)
Hemimorphite			10.0	0.06	< dl	1.4	< dl	2.0	1.9		< dl	< dl		158		395
	(< 10)	–	(100)	(10)	–	(10)	(< 10)	(10)	(10)	(100)	–	–	–	(> 100)	(10)	(> 100)
Olivine			50	< dl	0.2	1.65	10.8	64.2	3.6		0.7	0.27		34.3		69
	(10)	–	(> 10)	(tr)	(tr)	(10)	(> 10)	(100)	(10)	(100)	(10)	(tr)	–	(100)	(< 10)	(100)
Spurrite			245	< dl	< dl	0.5	< dl	18.5	< dl		< dl	< dl		< dl		79.5
	(< 10)	–	(100)	(tr)	–	(10)	(10)	(10)	(< 10)	–	–	–	–	(< 10)	(100)	(> 100)
Tephroite			7.5	< dl	< dl	0.5	100.1	12.0	340		< dl	< dl		1.35		115.5
	(10)	–	(10)	(tr)	–	(< 10)	(100)	(100)	(> 100)	–	–	–	(10)	(10)	(10)	(100)
Willemite			23.0	< dl	< dl	< dl	< dl	0.4	42.0		< dl	< dl		217		60
	(< 10)	(< 10)	(> 10)	(tr)	–	(< 10)	(10)	(< 10)	(100)	(> 100)	–	(tr)	–	(> 100)	(10)	(100)
0.5% m/m PAA Soln.			0.35	< dl	< dl	< dl	< dl	< dl	< dl		< dl	< dl		10.5?	–	< dl
	–	–	–	(tr)	–	(tr)	(tr)	(tr)	–	–	–	–	–	(tr)	–	–
Detectable limit (dl)			0.05	0.03	0.1	0.1	0.2	0.03	0.05		0.1	0.1		0.02		4.0

Ultra-violet emission spectroscopy results are given in parentheses.

TABLE VI Classification of mineral extract soluble ion concentration

Mineral	Major elements		Minor elements
	> 100 ppm	100–10 ppm	< 10 > 1 ppm
Andradite		Si, Ca, Mg, Fe, Al	Cu, Mn, Zn
Gadolinite		Si, Zn, Fe, Pb, Al, B, Be	Mg, Ca, Mn, Cu
Gehlinite	Si, Al	Ca, Mg, Zn, Na, B	Fe, Mn, Cu, Pb
Hardystonite	Si, Ca	Na	Mn, Mg, Pb, Zn, Cu, Al
Hemimorphite	Si, Zn	Ca, B, Na	Mg, Mn, Al, Cu, Cd
Olivine		Si, Mg, Zn, Ca, Na, Fe	Mn, Cu, Ni, Pb, Cr, Al
Spurrite	Ca	Si, Mg	Cu, Al
Tephroite	Si, Fe, Mn	Mg, Al	Ca, Zn, Cu
Willemite	Zn, Na	Si, Ca, Mn	Al, Mg

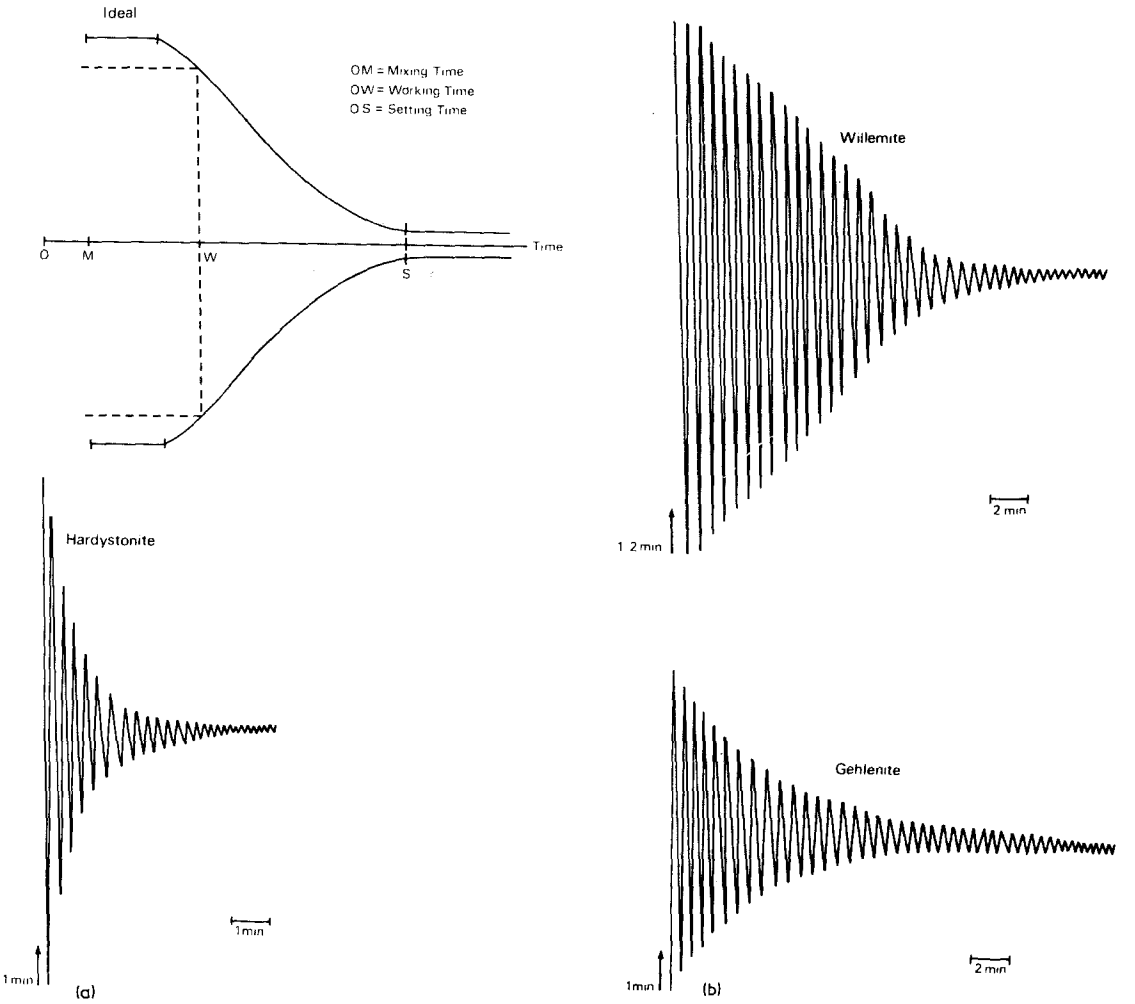

Figure 4 Rheometric traces of setting silicate mineral/PAA solution pastes (at 23° C).

are conveniently identified by DTA (Table III), since the major endothermic peaks observed between 725 to 850° C and 845 to 990° C can be attributed to decomposition of calcite and spurrite, respectively [18].

The nature of impurities in willemite and tephroite could not be determined with any certainty from their XRD patterns alone, but the detection of iron and magnesium in the sample of tephroite suggests the presence of picrotephroite ($(Mn, Mg)_2SiO_4$) and knebelite ($(Fe, Mn)_2SiO_4$). Major amounts of iron and manganese impurity

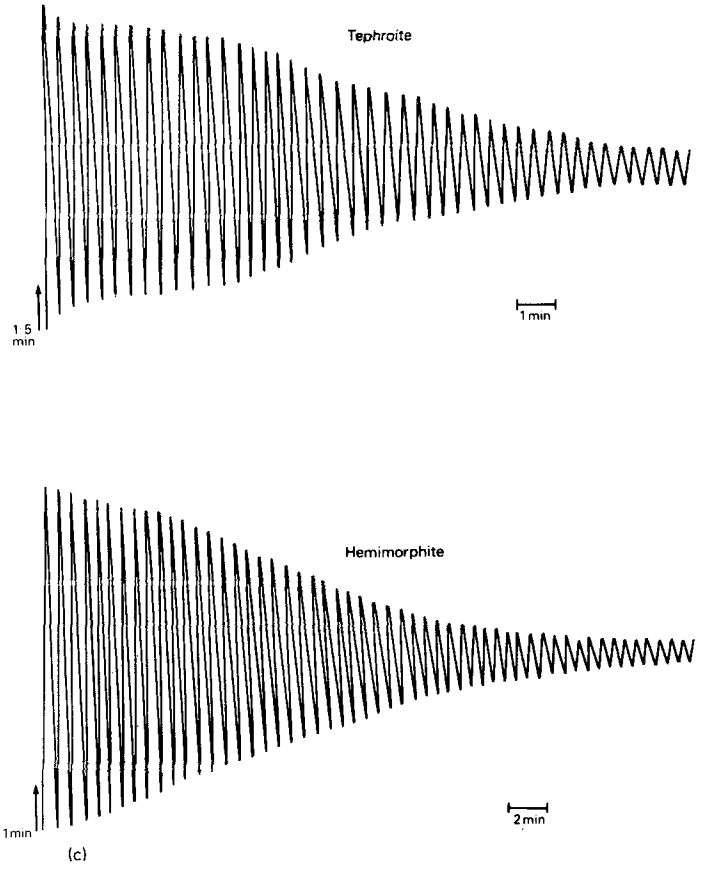

Figure 4 continued.

elements identified in willemite may be tentatively attributed to troostite ($(Zn, Mn)_2SiO_4$) and franklinite ($(Fe, Zn, Mn)O(Fe, Mn)_2O_3$) which are often associated with willemite in naturally occurring zinc ore deposits [21]. The composition of the gadolinite sample was more difficult to assess however. No impurities were found from inspection of its very weak XRD pattern, although there was poor agreement between experimental and published DTA results for this mineral (Table III).

Similar particle-size distribution for the mineral powders is to be expected, (Fig. 2) since they are structurally alike and were all comminuted in the same manner. Although the mean particle size and particle size distribution of these powders may influence the mechanical behaviour of cements made from them, the surface area available for protonic attack is considered to be a more important parameter in determining their reactivity towards polyacids. Since there appears to be no major difference between the specific surface areas of the various mineral powders (Table IV), it is inferred that any differences between the properties of cements made from these powders are a result of the inherent properties of the minerals themselves.

4.2. Acid decomposition of minerals

The comparison between results obtained using dilute PAA solution and more concentrated solution for cement formation appears to be valid at least during the early stages of acid attack and subsequent decomposition of the mineral particles, but the presence of excess water is likely to invalidate any such comparison at a later stage during setting. From a consideration of metallic cations extracted from the mineral powders by dilute PAA solution (Table VI) and the composition of the minerals before acid leaching (Table I), it is apparent that, in general, the major impurity elements were released by the acid in larger quantities than the minor impurity elements present but there were some anomalies. Iron, for example, was extracted from hemimorphite and willemite in only trace amounts and yet it was detected in significant concentrations in the

TABLE VII Infra-red absorptions of silicate minerals and silicate mineral cements. Frequencies in cm^{-1}

	Mineral literature [23]	Mineral	Cement	Assignment
Andradite			1700 sb	C=O stretch
		1650 w		Water
			1585 mb	C–O stretch salt
		1430 m		CO_3 impurity
			1405 mb	C–O stretch of salt (sym), C=O stretch, O–H
	1090–1085 bsh	1070 s	1060 s	Si–O stretch
	945–930 sh	940 sh	940 sh	
		900 m	895 m	
	895–887 vs	844 m	830 m	
	840–826 vs	824 w		CO_3 impurity
Gadolinite			1700 wsh	C=O stretch
			1540 sb	C–O stretch of salt (asym)
	1180 sh		1410 mb	C–O stretch of salt (sym)
	1100			
	1035 sb	1150–	1150–	Si–O stretch
	970 sh	750 sb	750 sb	
	802 vw			
	782 sh			
Gehlenite	3430		1640 wsh	Water
			1545 sb	C–O stretch of salt (asym)
			1440 sh	CH_2 bending
		1430 vwb		CO_3 impurity
			1405 m	C–O stretch of salts (sym)
			1333 w	CH_2 wagging, CH bending
		1120 sh	1120 sh	
	1020 sh	1055 w		Si–O stretching
	980 vs	1010 w	1010 w	
	922 vs	933 m		
	880 sh		920 w	
	860 sh	915 m		
	815 msh	860 m	850 w	CO_3 impurity
Hardystonite		1640 sh		Water
			1540 sb	C–O stretch of salt (asym)
		1430 vsb	1415 b	CO_3 impurity
			1415 sb	C–O stretch of salt (sym)
			1320 sh	CH_2 wagging, CH bending
	1038 sbsh	1060 s	1030 s	Si–O stretch
	1015 sh	974 s	965 m	
	971 s	920 s	905 s	
	916 vs	880 w	875 sh	
	895	848 s	835 m	CO_3 impurity
	838 s	842 sh		
Hemimorphite	3450			Water
			1700 sh	C=O stretch
	1635 w	1640 m		Water
			1560 svb	C–O stretch of salt (asym)
		1430 vs	1450 sh	CO_3 impurity
			1450 sh	CH_2 bending
			1400 m	C–O stretch of salt (sym)
			1315 w	CH_2 wagging, CH bending
	1090 s	1086 s	1084 sb	Si–O stretch
	1031 sh	935 s	930 s	
	940 vs	876 w	860 s	CO_3 impurity
	865 s	866 s		

s = strong; m = medium; w = weak; v = very; sh = shoulder, b = broad

TABLE VII (*contd.*)

	Mineral literature [23]	Mineral	Cement	Assignment
Olivine			1640 sh	Water
			1550 sb	C—O stretch of salt (asym)
			1440 sh	CH_2 bending
			1405 m	C—O stretch of salt (sym)
			1325 w	CH_2 wagging, CH bending
	1100 bsh		1060 s	
	1002 ssh	985 m	985 m	
	950 sh	958 m		
	898 s	885 s	885 s	
	848 sh	840 w	840 sh	
Spurrite		1785 w		
			Long tail	
			1750–	C=O stretch
			1620 sh	Water
			1520 w	C—O stretch of salt (asym)
		1514 w		
		1426 s	1420 sb	CO_3
			1420 sb	C=O stretch, OH
				C—O stretch of salt
		1326 w	945 svb	
		1316 w		
		1295 w		
		1274 m		
		1222 m		
		1222 m		
		1180–690 b band		CO_3 impurity
Tephroite			1700 sh	C=O stretch
			1540 sb	C—O stretch of salt (asym)
		1418 s		CO_3 impurity
			1400 s	C—O stretch of salt (sym)
			1320 w	CH_2 wagging, CH bending
		1090 w	1080 s	Si—O stretch
	978 sh	1030 s		
	968 ssh	960 s	950 w	
	935 sh	890 s	880 vw	CO_3 impurity
	865 vs	866 w	864 vw	
	820 ssh	824 w		
Willemite			1720 sh	C=O stretch
			1580 svb	C—O stretch of salt (asym)
		1420 sb		CO_3 impurity
			1440 sh	CH_2 bending
			1405 s	C—O stretch of salt (sym)
			1325 w	CH_2 wagging, CH bending
	1080 bsh	1115 sh	1115 sh	
	975 ssh	980 w	978 w	
	935 vs	928 w	930 w	
	905 vs	900 s	900 s	CO_3 impurity
	875 s	866 sh	865 w	
	852 sh			

s = strong; m = medium; w = weak; v = very; sh = shoulder; b = broad.

TABLE VIII Rheological characteristics of mineral–polyacid cement mixtures at 23° C

Cement composition		Powder/liquid ratio ($g\,ml^{-1}$)	Setting time (Gillmore needle)				Setting time (Rheometer)	Working time (Rheometer) (min)
			< 10 min	10–60 min	1–4 h	4–24 h		
Andradite	+ PAA	2:1	R	R	H*		soft after 24 h	8.24
	+ co-polymer	2:1					sealed cure at 23° C	–
Gadolinite	+ PAA	2:1	R	R	H		2 h 20 min	5.5
	+ co-polymer	2:1					2 days	7
Gehlenite	+ PAA	1:1	VR	H			48 min	0.5
	+ co-polymer	1.6:1					18 min	2.5
Hardystonite	+ PAA	1:1	H				6 min ⇌	0.25
	+ co-polymer	1:1					5 min	< 0.75
Hemimorphite	+ PAA	1:1	R	R	H		1 h 8 min	5.25
	+ co-polymer	1.3:1					27 min	2.9
Olivine	+ PAA	2:1	R	R	VR	H*	soft after 24 h	8.75
	+ co-polymer	2:1					sealed cure at 23° C	
							1 day	5.7
Spurrite	+ PAA	1:1	VR	H			–	1.75
	+ co-polymer	1:1					–	–
Tephroite	+ PAA	2:1	R	R	H		47 min	3.5
	+ co-polymer	2:1					23 min	2.0
Willemite	+ PAA	2:1	R	H			26 min	2.75
	+ co-polymer	2:1					8 min	1.7

PAA = 50% m/m aqueous poly(acrylic acid) solution
co-polymer = 50% m/m aqueous acrylic acid–itaconic acid co-polymer solution
* = hardened on drying out
R = rubbery
VR = very rubbery
H = set hard

TABLE IX Mechanical properties and solubility of mineral–polyacid cements

Cement composition	Powder/liquid ($g\,ml^{-1}$)	Samples stored 7 days at 100% r.h. + 7 days in water (23° C)			Samples stored 14 days at 100 r.h. (23° C)			
		Compressive strength (MPa)	Elastic modulus (MPa)	Strain at failure (%)	Compressive strength (MPa)	Elastic modulus (MPa)	Strain at failure (%)	Solubility in water (wt%)
Andradite + PAA	2:1	cement unstable			cement softened			complete disintegration
Gadolinite + PAA	2:1	40	1200	3.3	40	1220	3.3	0.02 stable
Gehlenite + PAA	1:1	1	3	28.4	6	20	26.5	2.4 softened
	(1.6:1)				(54)	(1200)	(4.5)	
Hardystonite + PAA	1:1	9	230	3.7	12	280	4.4	0.5 stable
	(1:1)				(52)	1210	(4.3)	
Hemimorphite + PAA	1:1	3	120	2.3	6	170	3.7	1.64 stable
	(1.3:1)				(9)	(280)	(3.2)	
Olivine + PAA	2:1	did not harden			did not harden			11.3 unstable
Spurrite + PAA	1:1	cement unstable			1	4	20.8	4.3 softened
	(1:1)				(31)	(860)	(3.6)	
Tephroite + PAA	2:1	cement unstable			cement softened			1.5 softened
	(2:1)				(4)	(150)	(2.7)	
Willemite + PAA	2:1	21	710	2.9	19	630	3.1	0.35 stable
	(2:1)				(11)	(300)	(3.7)	

Results in parentheses refer to mineral–itaconic acid/acrylic acid co-polymer mixtures containing tartaric acid.

original minerals. The presence of this iron in acid-stable mineral impurities is one possible explanation of this observation.

Some evidence for the stability of the mineral to dilute PAA solution also comes from weakening of X-ray reflection intensities of the mineral powders after reaction with dilute PAA solution. These results suggest an order of mineral stability towards PAA as:

andradite $\gg$ olivine, hemimorphite $>$

gadolinite, gehlenite, tephroite, willemite $>$

hardystonite, spurrite.

The greater stability of andradite is also demonstated by the low concentration of elements extracted from this mineral (Table V), and is attributed to the high bonding energy conferred by the strongly polarizing Fe (III) ion in the mineral lattice [22].

4.3. The setting reaction

Following the release of ions from acid-soluble mineral particles, the thickening and subsequent setting of the cement pastes are most probably the result of two concurrent effects. Poly(acrylic acid) in aqueous solution is largely un-ionized, and therefore assumes a tightly coiled spherical configuration. As the polyacid is progressively neutralized by metal cations in solution, the resulting negatively charged carboxylate ions along the chain cause it to unwind and leads to a thickening of the cement paste. Eventually the cations become ionically or covalently bound to the polyanion chains to form a highly reticulated metal–polyacrylate gel causing the cement mixture to set [6].

Infra-red spectroscopy demonstrates that polysalt gels are formed in each of the mineral–PAA compositions (Fig. 3, Table VII), and that the acid–base reaction proceeds to completion with gehlenite, hardystonite and olivine. Some mixtures notably those containing gadolinite, hemimorphite, spurrite, tephroite and willemite gave a small shoulder at 1710 cm^{-1} suggesting that a minor proportion of the PAA remained in its acid form. However, in the cement mixture made from andradite, a considerable amount of unreacted acid was detected which indicated only a small extent of reaction with the mineral. This observation is consistent with the inherent stability of andradite discussed earlier. In most cement spectra the metal–carboxylate asymmetric stretching band at about 1500 cm^{-1} is very strong and broad and is attributed to an overlap of multiple metal–polyacrylate absorptions of nearly equal frequencies [24]. Resolution of these bands was insufficient to enable positive identification of these salts or the nature of ion-binding, but it may be assumed that they largely originate from multivalent cations of the major elements leached from each mineral (Table VI). Carbonate, identified from the mineral spectra by a strong absorption at 1450 to 1410 cm^{-1} and another smaller band between 880 and 800 cm^{-1}, was evident in some of the minerals, e.g. hardystonite, hemimorphite, spurrite, tephroite and willemite [25]. It is significant, however, that these absorptions did not appear in the spectra of the hardened cements. In most of these mixtures, in particular those containing spurrite and hardystonite, considerable effervescence was apparent during mixing, and the carbon dioxide evolved resulted in the formation of a highly porous and friable cement.

4.4. Rheology of cement pastes

As in the case of other ionic polymer cements, the setting characteristics of mineral–cement pastes are likely to depend on a number of experimental variables including powder-to-liquid ratio, polyacid concentration, mineral particle size, temperature and to some extent the mixing technique adopted. More fundamental considerations, however, should relate to the rate and nature of cations extracted from the minerals and to their manner of association with the polyanion chains.

From a practical viewpoint, the available time for manipulation and shaping of a cement paste (i.e. working time) before setting commences is a particularly important property. It is evident from Table VIII, that most cement mixtures made using PAA passed through a rubbery condition, before setting.

However, compositions containing andradite and olivine gave anomalous results, since these mixtures remained rubbery when prevented from drying out. Their inability to set may be accounted for in different ways. It was shown earlier that andradite only partially reacts with PAA, thus limiting the extent of polysalt formation in this system. Most probably, therefore, the cement matrix consists of a lightly cross-linked polyacrylate gel, which imparts rubbery properties to the composite as a whole.

Olivine, however, was found to completely neutralize PAA, suggesting that the plastic behaviour of the resulting cement was influenced mainly by the nature of the salt-forming cations (i.e. principally Mg^{2+}, Ca^{2+} and possibly Zn^{2+}) and their mode of association with the polyanion chains. Based on an interpretation of infra-red spectrographic data, Crisp *et al.* [26] concluded that these ions are bound to a polyacrylate chain by electrostatic interactions of a non-directional nature, in contrast to ions such as Al^{3+} or Cu^{2+}, which are bound to specific sites on the chains by bonds having some covalent character. On application of a stress, ionically held cations are thought to permit the polyanionic chains to slip over one another resulting in some plasticity. It is likely that the mobility of ions in this way is enhanced by the presence of water in the cement. According to Ikegami [27, 28] water associated with a polyacrylate anion exists in individual spherical regions at localized charge sites, which tend to overlap as the chain is neutralized to produce a cylindrical envelope of water around the macro-ion. Surrounding this layer where the electrical field of the charged chain is weaker, a second cylindrical region of water is present. Divalent metal ions such as Mg^{2+}, which are weakly attracted by the electrostatic field of the polyanion, do not displace the primary water layer, but remain mobile in the outer secondary hydration region. These ions are, therefore, separated from the ionic groups on the chain by a solvent barrier. The situation becomes somewhat analogous to the plasticization of thermoplastics where in this example water is acting as the plasticizer.

The working and setting times of cement mixtures containing gehlenite, hardystonite and spurrite were very short even at the low powder-to-liquid ratio employed in this study. However, significant improvements in manipulative and hardening properties of these and other mineral–cement systems are possible by using an acrylic acid/itaconic acid co-polymer solution, as an alternative to PAA solution (Table VIII). In some mixtures either the working time was prolonged, allowing easier mixing and an increase in the powder-to-liquid ratio, or the setting time was reduced to a more practicable value. This polyacid variant is known to give similar improvements in manipulative qualities of glass–ionomer cement formulations [29].

4.5. Mechanical properties of hardened cements

The low strength and stiffness of most set and hardened mineral-cements (Table IX) may be largely attributed to their considerable porosity. In cements made from willemite, for example, a "true" porosity of 36% has been measured [1]. Clearly much of this porosity results from entrainment of CO_2 evolved during mixing, although even in carbonate-free *ortho-* and *pyro-*silicate minerals some voiding would be expected. It was inferred earlier that during setting of a cement paste complete erosion at the surface of the mineral particles is accompanied by neutralization and progressive thickening of the polymer phase.

As neutralization continues it becomes increasingly difficult, therefore, for matrix material to occupy space left by dissolved mineral particles, so that ultimately voiding occurs at the particle–matrix interface. In contrast, following the acid-decomposition of alumino-silicate (ASPA) glass powders, a siliceous hydrogel is formed at the surface of the particles, the latter retaining most of their initial volume. As a consequence, the porosity of cements made from these glasses is low, of the order of 5% [1].

The mechanical behaviour of mineral-cements is also influenced by the effectiveness of each mineral powder as a particulate filler. Improved composite properties are expected to result from using particles of high inherent strength and stiffness, which also exhibit some degree of either mechanical or chemical bonding to the surrounding gel matrix. Factors affecting the properties of the polysalt matrix, such as the extent of cross-linking and the nature and strength of ion-binding to polyanion chains, may also be pertinent. In this respect, the choice of polyacid appears to be particularly important. Results shown in Table IX, for example, show that for cements made from gehlenite, hardystonite and spurrite significant improvements in mechanical properties can be obtained by replacing PAA by an itaconic acid–acrylic acid co-polymer solution containing added tartaric acid.

4.6. Hydrolytic stability

The stability of mineral-cements towards water is primarily determined by the resistance to hydrolysis of the polyacid gel matrix formed during

setting. The observed variations in the solubility of polyacrylate salt gels containing different cations have been accounted for in a number of ways [30] which involve fundamental considerations of the properties of the cation, such as its ionic potential and its tendency to form complexes with a polyacrylate anion, as well as thermodynamic aspects including heats of hydration and ligation in gel formation and the extent of ligand field stabilization in gel complexes. Attempts to relate stability constant data for metal ion-polyacid complexes in dilute solution to the hydrolytic stability of ionic polymer cements, have shown some promise. For example, the greater solubility observed for cement mixtures made from MgO–PAA compared to ZnO–PAA [19], is in accordance with the reported stability constants ($-\log B_{av}$) of 3.8 and 3.0 for magnesium and zinc poly(acrylate), respectively [31].

Although the situation regarding most mineral-cements is complicated by the variety of cations extracted from each mineral (Table VI), some useful conclusions can nevertheless be drawn. Cements made from minerals rich in zinc (e.g. willemite and hemimorphite) are usually resistant to water, (Table IX), again demonstrating the stability of the zinc–polyacrylate gel matrix. By contrast, Ca^{2+} is less firmly held to polyacrylate chains and is more readily hydrolysed in an aqueous environment, accounting for the observed softening of the cement made from spurrite. In this respect the anomalous result obtained with hardystonite (of similar composition to spurrite,) is probably due to stabilization of the matrix by the small amounts of Cu^{2+} and Zn^{2+} impurity ions present in the sample.

Two possible mechanisms for hydrolysis have been proposed, one involving replacement of COO^- by OH^- and the other by H_2O ligands. In either case such substitution would result in a reduction in the strength of ionic binding followed by disruption of the metal-ion polyacrylate gel [32].

5. Conclusions

(1) During the initial stages of a cement-forming reaction *ortho-* and *pyro*-silicate mineral powders are decomposed by PAA solution, but by differing amounts. Hardystonite, for example is almost totally soluble, whereas andradite is only partially attacked due to its greater crystal stability.

(2) Cations which are released into solution vary according to the composition and reactivity of each mineral. These ions combine with polyacrylate chains to form multiple polysalts and cause the cement mixture to set to a rubbery or hard brittle mass, depending on the extent of reaction and the nature of the cations.

(3) The low compressive strength and stiffness of these solids in relation to other ionic polymer cements is attributed to their high porosity and also to the inherent weakness of the residual powder filler.

(4) The behaviour of the cements in water, however, is determined by the resistance to hydrolysis of the metal ion–polyacrylate matrix. In particular, high stability is observed in cements made from zinc-containing minerals such as willemite and hemimorphite.

(5) The replacement of PAA by an acrylic acid/itaconic acid co-polymer solution, containing tartaric acid, leads to significant improvement, both in the manipulative qualities of cement pastes and the mechanical properties of hardened mixtures.

References

1. J. ELLIOTT, L. HOLLIDAY and P. R. HORNSBY, *Brit. Polym. J.* 7 (1975) 297.
2. A. D. WILSON, *ibid.* 6 (1974) 165.
3. D. C. SMITH, *Brit. Dent. J.* 125 (1968) 381.
4. A. JURECIC, Canadian Patent no. 909 414, September (1972).
5. A. D. WILSON and B. E. KENT, British Patent no. 1 316 129, May (1973).
6. S. CRISP and A. D. WILSON, in "Ionic Polymers", edited by L. Holliday, (Applied Science Publishers, London, 1975) Ch. 4.
7. B. E. KENT and A. D. WILSON, *Brit. Dent. J.* 135 (1973) 322.
8. A. D. WILSON, in "Scientific Aspects of Dental Materials", edited by J. A. Fraunhofer (Butterworths, London, 1975) p. 211ff.
9. J. W. MCLEAN, and A. D. WILSON, *Austral. Dent. J.* 22 (1977) 31.
10. S. CRISP, A. D. WILSON, J. H. ELLIOTT and P. R. HORNSBY, *J. Appl. Chem. Biotechnol.* 27 (1977) 369.
11. British Standards Specifications for Dental Silicate Cement and Dental Silicophosphate Cement, Part 2, BS 3365 (1971).
12. C. G. PLANT, I. H. JONES, and H. J. WILSON, *Brit. Dent. J.* 133 (1972) 21.
13. C. R. ORCEL, *Acad. Sci. Paris* 236 (1953) 1052.
14. R. C. MACKENZIE "Scifax-Differential Thermal Analysis Data Index" (Cleaver-Hume Press, London, 1962).
15. A. J. KAUFFMAN and E. D. DILLING, *Econ. Geol.* 45 (1950) 222.
16. R. C. MACKENZIE, (Ed.) "Differential Thermal

Investigation of Clays" (London Mineralogical Society, 1957).
17. G. T. FAUST, *Amer. Mineral.* **36** (1951) 795.
18. S. CROSS, *Israel. J. Chem.* **9** (1971) 601.
19. P. R. HORNSBY, PhD Thesis, Brunel University, (1977).
20. A. D. WILSON, S. CRISP and A. J. FERNER, *J. Dent. Res.* **55** (1976) 489.
21. E. S. DANA, "A Textbook of Mineralogy", revised by W. E. Ford, 4th edn. (Wiley, New York and London, 1966).
22. H. MASE, *J. Chem. Soc. Japan* **34** (1961) 214.
23. J. A. GADSEN, "I.R. Spectra of Minerals and Related Inorganic Compounds" (Butterworths, London, 1975).
24. K. NAKAMOTO, "Infra-red spectra of Inorganic and Co-ordination Compounds", 2nd edn. (Wiley-Interscience, New York and London, 1970).
25. J. ZUSSMAN, (Ed.), "Physical Methods in Determinative Mineralogy" (Academic Press, New York and London, 1967).
26. S. CRISP, H. J. PROSSER and A. D. WILSON, *J. Mater. Sci.* **11** (1976) 36.
27. A. IKEGAMI, *J. Polymer Sci.* **A2** (1964) 907.
28. *Idem, Biopolymers* **6** (1968) 431.
29. S. CRISP, A. J. FERNER, B. G. LEWIS and A. D. WILSON, *J. Dentistry* **3** (1975) 125.
30. A. L. READER and K. A. HODD, *Brit. Polymer. J.* **8** (1976) 131.
31. H. P. GREGOR, L. B. LUTTINGER and E. M. LOEBL, *J. Phys. Chem.* **59** (1955) 990.
32. A. D. WILSON and S. CRISP, *Brit. Polym. J.* **7** (1975) 279.

Received 26 April and accepted 17 May 1979.